International Journal of Engineering

Journal Homepage: www.ije.ir

Non-linear Thermo-mechanical Bending Behavior of Thin and Moderately Thick Functionally Graded Sector Plates Using Dynamic Relaxation Method

M.E. Golmakani*[a], M. Kadkhodayan[b]

[a] *Department of Mechanical Engineering, College of Engineering, Mashhad Branch, Islamic Azad University, Mashhad, Iran*
[b] *Department of Mechanical Engineering, Ferdowsi University of Mashhad, Mashhad, Iran*

PAPER INFO

Paper history:
Received 31 May 2015
Received in revised form 23 May 2016
Accepted 02 June 2016

Keywords:
Non-linear Bending
Functionally Graded Materials
Sector Plate
Thermo-mechanical Behavior
Dynamic Relaxation Method

ABSTRACT

In this study, nonlinear bending of solid and annular functionally graded (FG) sector plates subjected to transverse mechanical loading and thermal gradient along the thickness direction is investigated. Material properties are varied continuously along the plate thickness according to power-law distribution of the volume fraction of the constituents. According to von-Karman relation for large deflections, the two set of highly coupled nonlinear equilibrium equations are derived based on both first order shear deformation theory (FSDT) and classical plate theory (CPT). The dynamic relaxation (DR) method in conjunction with the finite difference discretization technique is used to solve the nonlinear equilibrium equations. To demonstrate the efficiency and accuracy of the present solution, some comparison studies are carried out. Effects of material grading index, boundary conditions, sector angles, thickness-to-radius ratio and thermal gradient are studied in detail. Also, to consider the effect of shear deformation and nonlinearity on the results, some linear and nonlinear analyses are carried out based on both CPT and FSDT for different thickness-to-radius ratios and boundary conditions.

***doi**: 10.5829/idosi.ije.2016.29.06c.00*

1. INTRODUCTION

The sector plates combine light weight and high load-carrying capacity, economy and technological effectiveness, so they get extensive applications in all fields of engineering such as airplane, nuclear, aerospace and marine structures [1]. Because of the both theoretical interest and practical importance for the design purposes, some researchers have carried out linear analysis of isotropic and orthotropic sector plates [2-8]. The governing equations of sector plates undergoing moderately large deflections are more complicated than the governing equations of the rectangular plates and are not amenable to closed form or exact solutions and, finite element, finite difference etc., are used as a necessity [9]. In spite of being well established numerical methods, non-linear studies pertaining to isotropic sector plates are quite limited in extent [10-12]. Recently, the development of a new class of materials known as ‘‘functionally graded materials” (FGMs) in which the material properties change continuously in one or more directions consistent with a specific profile became significant. These non-homogeneous composite materials were first established by some researchers in Japan in 1984 [13]. FGMs are mainly manufactured by depositing ceramic layers on a metallic substrate or by high speed centrifugal casting [14]. Some studies have been considered static small deflection analysis of functionally graded circular and sector plates. Nosier and Fallah [15] reformulated the governing equations of the first-order shear deformation plate theory for FG circular plates into those describing the interior and edge-zone problems. They presented analytical solutions for axisymmetric and asymmetric bending behavior of functionally graded circular plates under mechanical and thermal loadings. Using a perturbation technique in conjunction with Fourier series method, Nosier and Fallah [16, 17] investigated the non-linear axisymmetric and asymmetric bending behavior of FG circular plates with various boundary conditions under

*Corresponding Author’s Email: *m.e.golmakani@mshdiau.ac.ir* (M.E. Golmakani)

Please cite this article as: M.E. Golmakani, M. Kadkhodayan, Non-linear Thermo-mechanical Bending Behavior of Thin and Moderately Thick Functionally Graded Sector Plates Using Dynamic Relaxation Method, International Journal of Engineering (IJE), TRANSACTIONS C: Aspects Vol. 29, No. 6, (June 2016)

mechanical and thermal loadings. By reformulating the governing equations of the first-order theory into those describing the interior and edge-zone problems of the plate, Nosier and Fallah [18] presented closed-form solutions for bending analysis of thermo-mechanical loaded FG circular sector plates with simply supported radial edges and various types of constraints for circular edges. Jomehzadeh et al. [19], Sahraee [20], Aghdam et al. [21] studied small deflection behavior of FG sector plate based on first order shear deformation theory (FSDT). Saidi et al. [22] decoupled the five highly coupled partial differential equations of FG solid sector plate under static loading using the boundary layer function and obtained analytical solutions for linear analysis of FG sector plates with various boundary conditions. This method is previously used by Nosier and coworkers [23, 24] for decoupling the highly coupled partial differential equations governing the small deflection of circular and sectorial plates. Using multi-term extended Kantorovich method, Mousavi and Tahani [25] analysed small deflection behavior of radially functionally graded (RFG) sector plates based on FSDT. Similar linear analysis is also conducted by Fereidoon et al. [26] for isotropic and RFG sector plates using the EKM and CPT. Until now, the various types of analytical solution methods have been applied for considering the linear bending and buckling analyses of FG plate [27-29]. Recently, authors [30-32] using the dynamic relaxation (DR) method together with the finite difference discretization technique investigated axisymmetric large deflection analysis of circular and annular FG plates/disks under thermo-mechanical loadings. But, according to the best knowledge of the authors, no work has been reported concerned with the large deflection thermoelastic analysis of moderately thick solid/annular functionally graded sector plates based on both CPT and FSDT. In the present paper, in order to fill this gap the linear and nonlinear bending formulation of moderately thick solid and annular FG sector plates under thermal and mechanical loadings are derived and solved based on both CPT and FSDT. Along this way, to consider the shear deformation effects, large deflection of FG sector plate has been analyzed for different thickness-to-radius ratios based on CPT and FSDT. The plate with various boundary conditions (simply supported and clamped) was subjected to uniform pressure loading and thermal gradient through the thickness. The DR method along with the finite difference discretization technique is employed to solve the equilibrium equations. Finally, in the parametric study the effects of material composition, thickness-to-radius ratio, shear deformation, boundary conditions and thermal gradient as well as the plate geometry parameters on the nonlinear thermoelastic response of the FGM plate are considered in detail. Furthermore, some studies are carried out to consider the effect of various parameters on the differences between the linear and nonlinear bending behaviors of FG sector plates based on CPT and FSDT.

2. GOVERNING EQUATIONS

Elastic solid and annular FG sector plates with the thickness, sector angle, inner and outer radiuses of h, α, r_i and r_o, respectively, subjected to a transverse uniform loading q and thermal gradient ΔT through the thickness are considered here. The geometry, loading and coordinate system of the solid and annular FG sector plates are shown in Figure 1(a, b), respectively. Based on the FSDT assumptions, displacement field in polar coordinates can be defined as:

$$\begin{aligned} U(r,\theta,z) &= u(r,\theta)+z\varphi_r(r,\theta),\\ V(r,\theta,z) &= v(r,\theta)+z\varphi_\theta(r,\theta),\\ W(r,\theta,z) &= w(r,\theta), \end{aligned} \tag{1}$$

where U, V and W are displacement fields while u, v and w are displacement components of the mid-surface in the r, θ and z directions, respectively. Moreover, φ_r and φ_θ are rotations of tangents with respect to the middle surface. Substituting Equation (1) into the von-Karman strain-displacement relations gives the following expressions [12]:

$$\begin{cases} \varepsilon_r = \varepsilon_r^0 + z\kappa_r = \dfrac{\partial u}{\partial r} + \dfrac{1}{2}\left(\dfrac{\partial w}{\partial r}\right)^2 + z\dfrac{\partial \varphi_r}{\partial r},\\ \varepsilon_\theta = \varepsilon_\theta^0 + z\kappa_\theta = \dfrac{1}{r}\left(u+\dfrac{\partial v}{\partial \theta}\right) + \dfrac{1}{2r^2}\left(\dfrac{\partial w}{\partial \theta}\right)^2 + \dfrac{z}{r}\dfrac{\partial \varphi_\theta}{\partial \theta} + z\dfrac{\varphi_r}{r},\\ \varepsilon_{r\theta} = \varepsilon_{r\theta}^0 + z\kappa_{r\theta} = \dfrac{1}{r}\left(\dfrac{\partial u}{\partial \theta} - v\right) + \dfrac{\partial v}{\partial r} + \dfrac{1}{r}\left(\dfrac{\partial w}{\partial r}\right)\left(\dfrac{\partial w}{\partial \theta}\right) + \dfrac{z}{r}\dfrac{\partial \varphi_r}{\partial \theta}\\ + z\dfrac{\partial \varphi_\theta}{\partial r} - z\dfrac{\varphi_\theta}{r}, \varepsilon_{rz} = \varepsilon_{rz}^0 = \varphi_r + \dfrac{\partial w}{\partial r}, \varepsilon_{\theta z} = \varepsilon_{\theta z}^0 = \varphi_\theta + \dfrac{1}{r}\dfrac{\partial w}{\partial \theta}. \end{cases} \tag{2}$$

where $(\varepsilon_r^0, \varepsilon_\theta^0, \varepsilon_{r\theta}^0, \varepsilon_{rz}^0, \varepsilon_{\theta z}^0)$ are the membrane strains, and $(\kappa_r, \kappa_\theta, \kappa_{r\theta})$ are the flexural (bending) strains, known as the curvatures [33]. The equations are obtained from a consideration of translational equilibrium in r, θ and z directions and rotational equilibrium about the r and θ axes.

$$\begin{cases} \dfrac{\partial N_r}{\partial r} + \dfrac{1}{r}\dfrac{\partial N_{r\theta}}{\partial \theta} + \dfrac{1}{r}(N_r - N_\theta) = 0,\\ \dfrac{\partial N_{r\theta}}{\partial r} + \dfrac{1}{r}\dfrac{\partial N_\theta}{\partial \theta} + \dfrac{2}{r}N_{r\theta} = 0,\\ \dfrac{\partial Q_\theta}{r\partial \theta} + \dfrac{Q_r}{r} + \dfrac{\partial Q_r}{\partial r} + N_\theta\left(\dfrac{1}{r}\dfrac{\partial w}{\partial r} + \dfrac{1}{r^2}\dfrac{\partial^2 w}{\partial \theta^2}\right)\\ + N_r\dfrac{\partial^2 w}{\partial r^2} + 2N_{r\theta}\left(\dfrac{1}{r}\dfrac{\partial^2 w}{\partial r\partial \theta} - \dfrac{1}{r^2}\dfrac{\partial w}{\partial \theta}\right) + q = 0,\\ \dfrac{\partial M_r}{\partial r} + \dfrac{\partial M_{r\theta}}{r\partial \theta} + \dfrac{M_r - M_\theta}{r} - Q_r = 0,\\ \dfrac{\partial M_\theta}{r\partial \theta} + \dfrac{\partial M_{r\theta}}{\partial r} + \dfrac{2}{r}M_{r\theta} - Q_\theta = 0, \end{cases} \tag{3}$$

where in-plane resultant forces N_r, N_θ and $N_{r\theta}$ and out of plane resultant forces and Q_r and Q_θ can be

defined by integrating corresponding stresses along the thickness as:

$$(N_r, N_\theta, N_{r\theta}) = \int_{-h/2}^{h/2} (\sigma_r, \sigma_\theta, \sigma_{r\theta}) dz,$$
$$(Q_r, Q_\theta) = k_s^2 \int_{-h/2}^{h/2} (\sigma_{rz}, \sigma_{\theta z}) dz, \tag{4}$$

In this work, according to [34-36], the shear correction factor k_s^2 is taken as 5/6. Figure 2 shows the 'force' system used to derive the following equilibrium equations (for more detail see [12]). Moreover, similar to Equation (4), the resultant moments M_r, M_θ and $M_{r\theta}$ are:

$$(M_r, M_\theta, M_{r\theta}) = \int_{-h/2}^{h/2} (\sigma_r, \sigma_\theta, \sigma_{r\theta}) z dz. \tag{5}$$

Furthermore, stress- strain relationship for FG sector plates can be written as:

$$\sigma_r = \frac{E(z)}{(1-\nu^2)}\left[\varepsilon_r + \nu\varepsilon_\theta - \alpha\Delta T\right], \sigma_\theta = \frac{E(z)}{(1-\nu^2)}\left[\varepsilon_\theta + \nu\varepsilon_r - \alpha\Delta T\right],$$
$$\sigma_{r\theta} = \frac{E(z)}{2(1+\nu)}\varepsilon_{r\theta},\ \sigma_{rz} = \frac{E(z)}{2(1+\nu)}\varepsilon_{rz},\ \sigma_{\theta z} = \frac{E(z)}{2(1+\nu)}\varepsilon_{\theta z}, \tag{6}$$

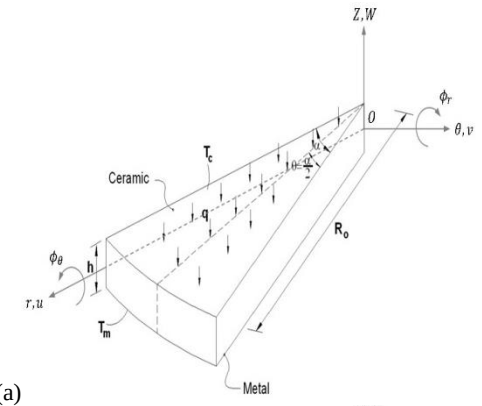

(a)

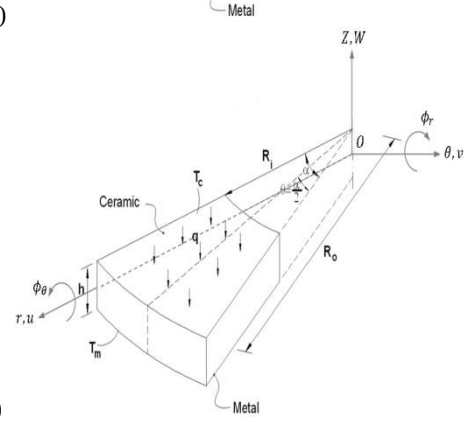

(b)

Figure 1. The geometry and coordinate system of the, (a) solid and (b) annular FG sector plates.

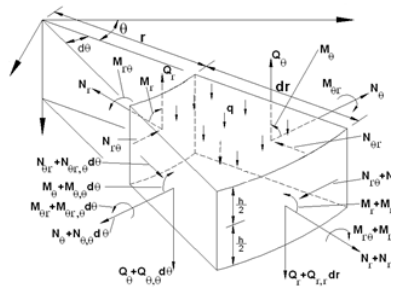

Figure 2. The internal and external forces and moments acting on the cross section areas of the sector plate.

where ν is the Poisson ratio and is considered to be constant [37]. Moreover, E is Young modulus and is assumed to vary continuously throughout the thickness of the plate, according to the volume fraction of the constituent materials based on a power law function as [38]:

$$E(z) = (E_c - E_m)\left(\frac{2z+h}{2h}\right)^n + E_m, \tag{7}$$

where subscripts c and m denote ceramic and metal, respectively, z is distance from mid-surface of the plate along z axis ($-h/2 \le z \le h/2$) and n is the volume fraction exponent of a FGM. According to this distribution, the bottom surface ($z = -h/2$) of the functionally graded plate is pure metal, and the top surface ($z = h/2$) is pure ceramic. Using (2), (4), (5) and (6) gives the following constitutive relations:

$$\begin{bmatrix} N_r \\ N_\theta \\ N_{r\theta} \\ M_r \\ M_\theta \\ M_{r\theta} \end{bmatrix} = \begin{bmatrix} A_{11} & A_{12} & 0 & B_{11} & B_{12} & 0 \\ A_{12} & A_{22} & 0 & B_{12} & B_{22} & 0 \\ 0 & 0 & A_{66} & 0 & 0 & B_{66} \\ B_{11} & B_{12} & 0 & D_{11} & D_{12} & 0 \\ B_{12} & B_{22} & 0 & D_{12} & D_{22} & 0 \\ 0 & 0 & B_{66} & 0 & 0 & D_{66} \end{bmatrix} \begin{bmatrix} \varepsilon_r^0 \\ \varepsilon_\theta^0 \\ \varepsilon_{r\theta}^0 \\ \kappa_r \\ \kappa_\theta \\ \kappa_{r\theta} \end{bmatrix} - \begin{bmatrix} N_r^T \\ N_\theta^T \\ 0 \\ M_r^T \\ M_\theta^T \\ 0 \end{bmatrix} \tag{8}$$

$$Q_r = k_s^2 A_{66}\left(\varphi_r + \frac{\partial w}{\partial r}\right),$$
$$Q_\theta = k_s^2 A_{66}\left(\varphi_\theta + \frac{1}{r}\frac{\partial w}{\partial \theta}\right), \tag{9}$$

where the stiffness coefficients are defined as:

$$(A_{11}, B_{11}, D_{11}) = \int_{-h/2}^{h/2} \frac{E(z)}{1-\nu^2}(1, z, z^2) dz,$$
$$(A_{12}, B_{12}, D_{12}) = \int_{-h/2}^{h/2} \frac{\nu E(z)}{1-\nu^2}(1, z, z^2) dz, \tag{10}$$
$$(A_{66}, B_{66}, D_{66}) = \int_{-h/2}^{h/2} \frac{E(z)}{2(1+\nu)}(1, z, z^2) dz.$$

It is noticed that because of gradually varying the composition of the constituent materials in the thickness direction only and in-plane isotropic properties of the

FG plate, the statements $A_{11}=A_{22}.B_{11}=B_{22},D_{11}=D_{22}$ are taken to be account for the extensional, extension-bending coupling, and bending stiffness matrices *A*, *B*, *D*, respectively. The membrane forces and bending moments induced by thermal loading per unit edge length in Equation (8) can be computed as:

$$N_r^T=N_\theta^T=\int_{-h/2}^{h/2}\frac{E(z)}{1-\nu}\alpha(z)T(z)dz,$$
$$M_r^T=M_\theta^T=\int_{-h/2}^{h/2}\frac{E(z)}{1-\nu}\alpha(z)T(z)zdz, \tag{11}$$

It is notable that expressions $N_r^T=N_\theta^T$ and $M_r^T=M_\theta^T$ are considered owing to the in-plane isotropic material properties of the FG plate. For thermal loading problems, it is assumed that the temperature variation is only along the thickness direction. The one-dimensional heat transfer equation for the z-direction is given by:

$$-\frac{d}{dz}\left(K(z)\frac{dT(z)}{dz}\right)=0, \tag{12}$$

where the thermal conductivity coefficient $K(z)$ in Equation (12) obeys the simple rule of mixture as follows:

$$K(z)=(K_c-K_m)\left(\frac{2z+h}{2h}\right)^n+K_m. \tag{13}$$

Hence, it is easy to obtain the temperature function $T(z)$ from Equation (12) as follows [39]:

$$T(z)=T_m+(T_c-T_m)\int_{-h/2}^{z}\frac{dz}{K(z)}\Big/\int_{-h/2}^{h/2}\frac{dz}{K(z)}, \tag{14}$$

where $T=T_c$ at $z=h/2$ and $T=T_m$ at $z=-h/2$. It must be noted that $T(z)$ is measured from the stress free state $T_0=0^oC$. Substituting the resultant forces and moments obtained from Equations (8) and (9) into Equation (3), the five equilibrium equations are obtained in terms of the displacement field. For the sake of brevity, only the first equation is given as below

$$\begin{aligned}
&A_{11}\left(\frac{\partial^2 u}{\partial r^2}+\frac{\partial^2 w}{\partial r^2}\frac{\partial w}{\partial r}+\nu\left(\frac{1}{r}\frac{\partial u}{\partial r}-\frac{u}{r^2}+\frac{1}{r}\frac{\partial^2 v}{\partial r\partial\theta}-\frac{1}{r^2}\frac{\partial v}{\partial\theta}-\frac{1}{r^3}\left(\frac{\partial w}{\partial\theta}\right)^2+\frac{1}{r^2}\frac{\partial^2 w}{\partial r\partial\theta}\frac{\partial w}{\partial\theta}\right)\right)\\
&+B_{11}\left(\frac{\partial^2\varphi_r}{\partial r^2}-\frac{\nu}{r^2}\frac{\partial\varphi_\theta}{\partial\theta}+\frac{\nu}{r}\frac{\partial^2\varphi_\theta}{\partial r\partial\theta}-\frac{\nu\varphi_r}{r^2}+\frac{\nu}{r}\frac{\partial\varphi_r}{\partial r}\right)\\
&+\frac{A_{11}}{r}\left(\left(\frac{\partial u}{\partial r}+\frac{1}{2}\left(\frac{\partial w}{\partial r}\right)^2-\frac{u}{r}-\frac{1}{r}\frac{\partial v}{\partial\theta}-\frac{1}{2}\left(\frac{\partial w}{r\partial\theta}\right)^2\right)+\nu\left(\frac{u}{r}+\frac{1}{r}\frac{\partial v}{\partial\theta}+\frac{1}{2r^2}\left(\frac{\partial w}{\partial\theta}\right)^2-\frac{\partial u}{\partial r}-\frac{1}{2}\left(\frac{\partial w}{\partial r}\right)^2\right)\right)\\
&+\frac{B_{11}}{r}\left(\frac{\partial\varphi_r}{\partial r}+\frac{\nu}{r}\frac{\partial\varphi_\theta}{\partial\theta}+\frac{\nu\varphi_r}{r}-\frac{1}{r}\frac{\partial\varphi_\theta}{\partial\theta}+\frac{\varphi_r}{r}+\nu\frac{\partial\varphi_r}{\partial r}\right)\\
&+\frac{A_{66}}{r}\left(\frac{1}{r}\left(\frac{\partial^2 u}{\partial\theta^2}-\frac{\partial v}{\partial\theta}\right)+\frac{\partial^2 v}{\partial r\partial\theta}+\frac{1}{r}\frac{\partial^2 w}{\partial r\partial\theta}\frac{\partial w}{\partial\theta}+\frac{1}{r}\frac{\partial w}{\partial r}\frac{\partial^2 w}{\partial\theta^2}\right)\\
&+\frac{B_{66}}{r}\left(\frac{1}{r}\frac{\partial^2\varphi_r}{\partial\theta^2}+\frac{\partial^2\varphi_\theta}{\partial r\partial\theta}-\frac{1}{r}\frac{\partial\varphi_\theta}{\partial\theta}\right)=0,
\end{aligned} \tag{15}$$

In this paper, in order to consider the effect of shear deformations on the results, the computed results based on FSDT are compared with the ones obtained based on CPT. Thus, the large deflection analysis of the FG sector plate are carried out based on both FSDT and CPT. The three equations which describe the state of equilibrium in the presence of both in- and out-of plane deformations within CPT are given in [11, 33]:

It is clear that the main differences between FSDT and CPT are originated from the definition of displacement field of each theory. So that compared to the displacement field based on FSDT, the rotations of tangents with respect to the middle surface in CPT are: $\phi_r=-\partial w/\partial r$ and $\phi_\theta=-\partial w/r\partial\theta$. Therefore, the radial, tangential and twisting curvatures of Equation (8) are $-(\partial^2 w/\partial r^2)$, $-(1/r^2)(\partial^2 w/\partial\theta^2)-(1/r)(\partial w/\partial r)$ and $-(2/r)(\partial^2 w/\partial r\partial\theta)+(2/r^2)(\partial w/\partial\theta)$, respectively, based on CPT. Now, according to the described rotations and curvatures based on CPT, by replacing the displacement and strain fields of CPT in Equation (8) and the stiffness coefficients expressed in Equation (10) which is identical for both FSDT and CPT, the statement of the constitutive equations ($N_r,N_\theta,N_{r\theta},M_r,M_\theta,M_{r\theta}$) can be written based on the displacement field of CPT.

The equilibrium equations have to be accompanied by a set of boundary conditions which are here all-round clamped and simply supported. The constraints on the displacements and stress resultants/couples at the circumferential and radial plate edges imposed in each case are given as follows:

(a) On the radial edges ($\theta=0^o$ and $\theta=\alpha$) for simply supported edges:

$$u=v=w=\varphi_r=M_\theta=0, \tag{16}$$

for clamped edges:

$$u=v=w=\varphi_r=\varphi_\theta=0, \tag{17}$$

(b) On the circumferential edges ($r=r_i$ and $r=r_o$) for simply supported edges:

$$u=v=w=\varphi_\theta=M_r=0, \tag{18}$$

for clamped edges:

$$u=v=w=\varphi_r=\varphi_\theta=0, \tag{19}$$

For the sake of brevity, the boundary conditions of FG sector plate based on CPT are omitted, see [33].

3. NUMERICAL SOLUTION OF THE SECTOR PLATE EQUATIONS

The five non-linear equilibrium equations which show the large deflection response of a FG sector plate under

combined thermal and mechanical load is very complex and is not amenable to a closed form solution. Among the numerical solution methods like finite element, finite difference, finite strip, relaxation, etc., the dynamic relaxation (DR) technique [40] in conjunction with a central finite difference discretization scheme has been used here to solve the nonlinear differential equations of the solid and annular FG sector plates. The DR algorithm has been selected for solving the governing equations of plate because of two reasons: (1) the equations of large deflection FG sector plate have not previously been solved by this method and also by any other technique and (2) the authors [30-32, 41, 42] and others [43-45] have demonstrated its effectiveness for elastic and elasto-plastic large deflection plate analysis. To solve the plate equations using DR method they are transformed from a boundary value problem to an initial value format to facilitate the integration of the governing equations via a simple time-stepping iterative procedure. The first stage of the transformation process is to render the equilibrium equations 'quasi-dynamic' by adding damping and inertia terms to their right-hand sides. Hence, the Equation (3) based on FSDT takes the following form:

$$\frac{\partial N_r}{\partial r}+\frac{1}{r}\frac{\partial N_{r\theta}}{\partial \theta}+\frac{1}{r}\left(N_r-N_\theta\right)=m_u\frac{d^2u}{dt^2}+c_u\frac{du}{dt} \tag{20}$$

Similarly, Equation (20) can be transformed to a quasi-dynamic equation based on CPT. The second stage of the process is to replace the velocity and acceleration terms introduced in Equation (20) by the following approximate relations:

$$\dot{X}^{n-\frac{1}{2}}=\left(X^n-X^{n-1}\right)/\tau^n, \tag{21}$$

$$\ddot{X}^n=(\dot{X}^{n+\frac{1}{2}}-\dot{X}^{n-\frac{1}{2}})/\tau^n. \tag{22}$$

where $X=u,v,w,\varphi_r,\varphi_\theta$ is the approximate solution vector at the nth iteration and τ is the increment of fictitious time. By substituting Equations (21) and (22) into the right-hand side of Equations (20), the velocity equations are obtained. For instance, the first velocity equations of FSDT are given as follows:

$$\dot{u}_i^{n+1/2}=\frac{2\tau^n}{2+\tau^n c_i^n}(m_{ii}^l)^{-1}\left(\frac{\partial N_r}{\partial r}+\frac{1}{r}\left(N_r-N_\theta\right)+\frac{1}{r}\frac{\partial N_{r\theta}}{\partial \theta}\right)_i^n+\frac{2-\tau^n c_i^n}{2+\tau^n c_i^n}\dot{u}_i^{n-1/2} \tag{23}$$

where $m_{ii}^l:[u,v,w,\varphi_r,\varphi_\theta]$ are elements of the diagonal fictitious mass matrices M. Here, to guarantee the numerical stability, the element of matrix M is determined by the Gershgörin theorem as (for more detail see [46, 47]):

$$m_{ii}^l\geq .25(\tau^n)^2\sum_{j=1}^{N}\left|k_{ij}^l\right|, \tag{24}$$

where k_{ij} is the element of the stiffness matrix K and is obtained by:

$$K=\frac{\partial P}{\partial X}. \tag{25}$$

Similar relation between M and m_{ii}^l is used for elements of diagonal fictitious damping matrices C and c_{ii}^l. By employing the Rayleigh principle for node i at the *nth* iteration, the instant critical damping factor can be computed as follows [46]:

$$c_i^n=2\left\{\frac{(x_i^n)^T p_i^n}{(x_i^n)^T m_{ii}^n x_i^n}\right\}^{1/2}. \tag{26}$$

Thus, different c values are introduced for each node to obtain the form used for DR as follows [46]:

$$c_{ii}=c_i m_{ii},\qquad i=1,\ldots,N \tag{27}$$

To calculate the displacements, the velocity equations are integrated after each time step as follows:

$$u^{n+1}=u^n+\tau^{n+1}\overset{o}{u}^{n+1/2} \tag{28}$$

Similar equations can be employed to obtain the other displacement components. After computing the displacement field and applying the boundary conditions, strains and resultant stresses can be calculated. For the sake of brevity, the DR algorithm which clearly explained in [31, 41] is omitted.

4. NUMERICAL RESULTS AND DISCUSSIONS

4. 1. Comparison study To demonstrate the efficiency and accuracy of the present solution, some illustrative examples were solved for linear/nonlinear bending of solid and annular FGM sector plates with different boundary conditions.

Example 1. In this section as a part of validation of our analysis, the present results for the linear behavior of moderately thick FG sector plates subjected to uniform transverse loading q are compared with those obtained by Ref. [21] based on FSDT. Comparisons between the results of present work and those obtained by Aghdam et al. [21] are shown in Figure 3 for the dimensionless deflection $\bar{W}=1000wE_c h^3/qr_o^4$. Again, it is clear that present results are in good agreement with the analytical solutions obtained by Aghdam et al. [21].

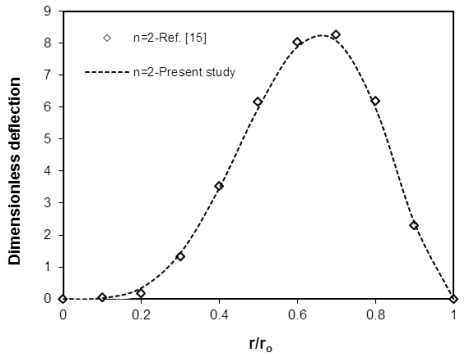

Figure 3. Comparisons between the present work and the results obtained by Aghdam et al. [21] for the dimensionless deflection ($\bar{W}$) along the radial direction ($\theta = \alpha / 2$).

Example 2. In this case, the DR solutions are compared with the ones reported by Fallah and Nosier [18] for the thermal bending response of functionally graded circular sector plates with simply supported boundary conditions. As shown in Figure 4, the obtained dimensionless deflections ($\bar{w} = w / h$) of the circular sector plate ($\alpha = 60^o, h / r_o = 0.1$) are in good consistency with those reported by Fallah and Nosier [18].

4. 2. Parametric Study Metal/ Aluminum and ceramic/ Zirconia system of FGM was considered in which the ceramic rich top surface maintained at $300^\circ C$, unless stated otherwise, and the metal rich bottom surface at $20^\circ C$ while the stress-free temperature is $T_0 = 0^\circ C$ [30]. The results are defined in terms of the following dimensionless quantities $\bar{u} = ur_o / h^2, \bar{M}_r = M_r r_o^2 / E_c h^4, \bar{N}_r = N_r r_o^2 / E_c h^3, \bar{w} = w / h$, $\bar{q} = q r_o^4 / E_c h^4$ which show the dimensionless radial displacement, radial moment, radial membrane force, deflection and load, respectively.

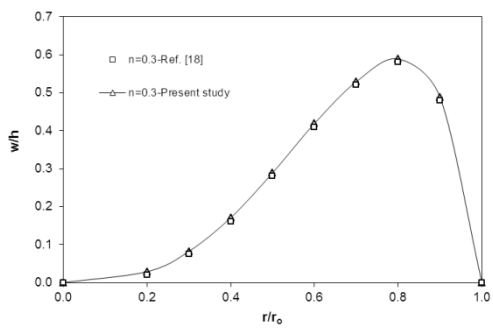

Figure 4. Comparisons between the DR solutions and those reported by Fallah and Nosier [18] for the thermal bending response of FG circular sector plates ($\alpha = \pi / 3$) with simply supported boundary conditions.

In the present work, a 60° sector plate with $r_o = 100mm$ and a thickness-to-radius ratio of $\lambda = 0.1, 0.15.02$ subjected to uniform transverse loading of $\bar{q} = 500$ and thermal loading $\Delta T = 300^\circ C$ is considered, unless stated otherwise. The ratio of the outer-to-inner radius for the annular plate was assumed as $r_i / r_o = 0.4$.

Figures 5 and 6 respectively show the vertical and radial displacements and radial forces and moments ($\bar{w}$, $\bar{u}$, $\bar{N}_r$ and $\bar{M}_r$) for clamped (CCCC) annular sector plate with $\lambda = 0.2$ subjected to uniform mechanical loading with different material grading indices *n*.

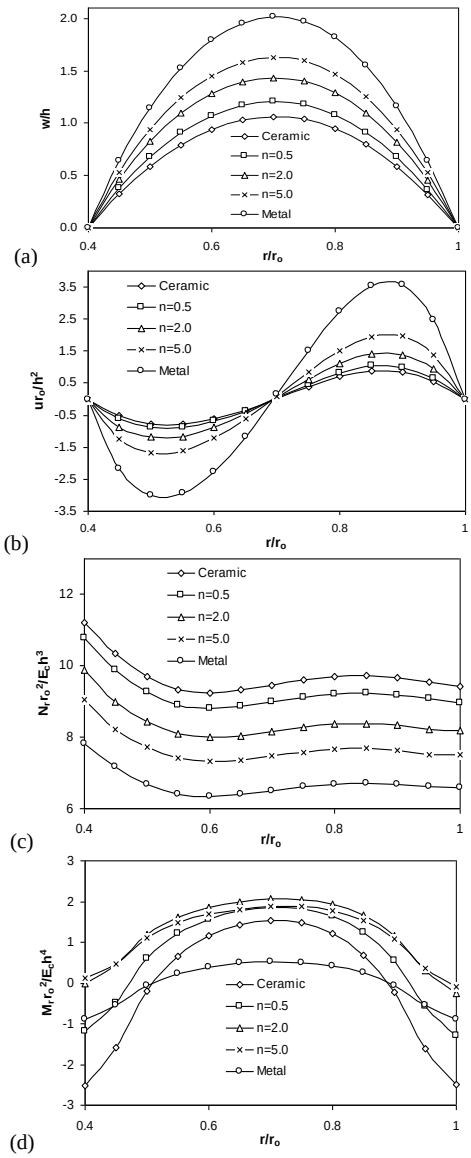

Figure 5. Effects of material grading index *n* on the (a) $\bar{w}$, (b) $\bar{u}$, (c) $\bar{N}_r$ and (d) $\bar{M}_r$ along the radial direction ($\theta = \alpha / 2$) of a CCCC annular sector plate.

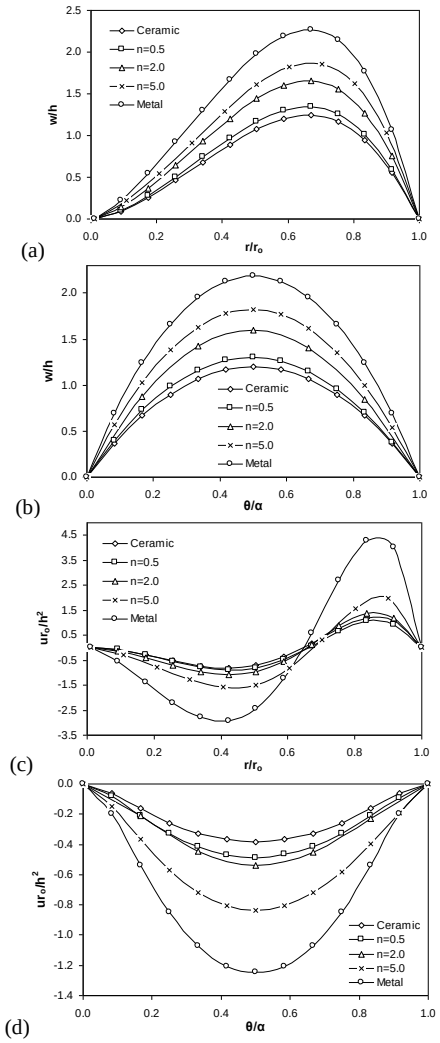

Figure 6. Variations of $\bar{w}$ (a), (b) and $\bar{u}$ (c), (d) along the radial ($\theta = \alpha/2$) and circumferential direction ($\bar{r} = 0.6$) of a SSS FG solid sector plate.

It is notable that Figures 5 and 6 are specified for $\theta = \alpha/2$ and $\bar{r} = 0.75$, respectively. As it is expected, increasing *n* and tendency of material properties toward metallic phase cause increasing of $\bar{w}$ and $\bar{u}$, while decrease of *n* increases $\bar{N}_r$. Moreover, variations of $\bar{M}_r$ (Figures 5(d) and 6(d)) imply that the minimum of $\bar{M}_r$ occurs at the center of homogenous metallic and ceramic plates and the variations of $\bar{M}_r$ in terms of *n* is not monotonic. Obviously, maximum amount of $\bar{N}_r$ and $\bar{M}_r$ take place at the inner edge and center of the plate, respectively.

The effect of nonlinearity on the maximum dimensionless deflection $\bar{w}_{\max}$ of the FG solid sector plate subjected to uniform mechanical loading with *n=1* and $\lambda = 0.2$ are considered in Figure 7 (a, b) for CCC

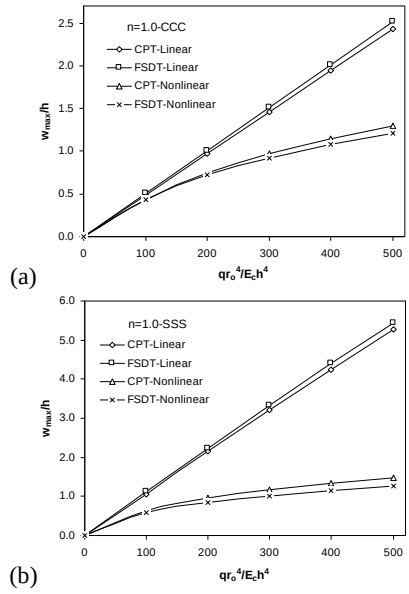

Figure 7. Comparisons of ($\bar{w}_{\max} = w_{\max}/h$) obtained by linear and nonlinear analyses based on both CPT and FSDT for (a) CCC and (b) SSS solid FG sector plate.

and SSS boundary conditions, respectively, based on both CPT and FSDT. As observed for both CCC and SSS boundary conditions, there is a huge amount of differences between the linear and nonlinear results predicted by CPT and FSDT.

5. Conclusions

Nonlinear bending behavior of solid and annular FG sector plates subjected to transverse mechanical loading and thermal gradient along the thickness direction is investigated. Material properties are varied continuously along the plate thickness according to power-law distribution of the volume fraction of the constituents. Based on von Karman theory for large deflection, non-linear equilibrium formulations were obtained based on CPT and FSDT. The DR numerical method combined with the finite difference discretization technique was employed to solve the highly coupled nonlinear equilibrium equations. Effects of material gradient constant, thermal loading, boundary conditions and different ratios of thickness-to-radius were studied. It was seen that unlike the linear analysis, the deflections obtained based on CPT had the larger values compared to FSDT for nonlinear behavior. While, with increase of thickness-to-radius ratios and shear deformation effects the larger amount of $\bar{w}$ was predicted by FSDT compared to CPT for nonlinear bending analysis of CCC FG sector plate.

6. REFERENCES

1. Ventsel, E. and Krauthammer, T., "Thin plates and shells: Theory: Analysis, and applications, CRC press, (2001).
2. Kobayashi, H. and Turvey, G.J., "Elastic small deflection analysis of annular sector mindlin plates", ***International Journal of Mechanical Sciences***, Vol. 36, No. 9, (1994), 811-827.
3. Aghdam, M., Mohammadi, M. and Erfanian, V., "Bending analysis of thin annular sector plates using extended kantorovich method", ***Thin-Walled Structures***, Vol. 45, No. 12, (2007), 983-990.
4. Kim, K. and Yoo, C.H., "Analytical solution to flexural responses of annular sector thin-plates", ***Thin-Walled Structures***, Vol. 48, No. 12, (2010), 879-887.
5. Harik, I.E., "Analytical solution to orthotropic sector", ***Journal of Engineering Mechanics***, Vol. 110, No. 4, (1984), 554-568.
6. Aghdam, M. and Mohammadi, M., "Bending analysis of thick orthotropic sector plates with various loading and boundary conditions", ***Composite Structures***, Vol. 88, No. 2, (2009), 212-218.
7. Cheung, M. and Chan, M., "Static and dynamic analysis of thin and thick sectorial plates by the finite strip method", ***Computers & Structures***, Vol. 14, No. 1, (1981), 79-88.
8. Lim, G. and Wang, C., "Bending of annular sectorial mindlin plates using kirchhoff results", ***European Journal of Mechanics-A/Solids***, Vol. 19, No. 6, (2000), 1041-1057.
9. Andakhshideh, A., Maleki, S. and Aghdam, M., "Non-linear bending analysis of laminated sector plates using generalized differential quadrature", ***Composite Structures***, Vol. 92, No. 9, (2010), 2258-2264.
10. Nath, Y., Sharda, H. and Sharma, A., "Non-linear analysis of moderately thick sector plates", ***Communications in Nonlinear Science and Numerical Simulation***, Vol. 10, No. 7, (2005), 765-778.
11. Salehi, M. and Turvey, G., "Elastic large deflection response of annular sector plates—a comparison of dr finite-difference, finite element and other numerical solutions", ***Computers & Structures***, Vol. 40, No. 5, (1991), 1267-1278.
12. Salehi, M. and Shahidi, A., "Large deflection analysis of elastic sector mindlin plates", ***Computers & Structures***, Vol. 52, No. 5, (1994), 987-998.
13. Koizumi, M., "Fgm activities in japan", ***Composites Part B: Engineering***, Vol. 28, No. 1, (1997), 1-4.
14. Hosseini-Hashemi, S., Akhavan, H., Taher, H.R.D., Daemi, N. and Alibeigloo, A., "Differential quadrature analysis of functionally graded circular and annular sector plates on elastic foundation", ***Materials & Design***, Vol. 31, No. 4, (2010), 1871-1880.
15. Nosier, A. and Fallah, F., "Reformulation of mindlin–reissner governing equations of functionally graded circular plates", ***Acta Mechanica***, Vol. 198, No. 3-4, (2008), 209-233.
16. Nosier, A. and Fallah, F., "Non-linear analysis of functionally graded circular plates under asymmetric transverse loading", ***International Journal of Non-Linear Mechanics***, Vol. 44, No. 8, (2009), 928-942.
17. Fallah, F. and Nosier, A., "Nonlinear behavior of functionally graded circular plates with various boundary supports under asymmetric thermo-mechanical loading", ***Composite Structures***, Vol. 94, No. 9, (2012), 2834-2850.
18. Fallah, F. and Nosier, A., "Thermo-mechanical behavior of functionally graded circular sector plates", ***Acta Mechanica***, Vol. 226, No. 1, (2015), 37-54.
19. Jomehzadeh, E., Saidi, A. and Atashipour, S., "An analytical approach for stress analysis of functionally graded annular sector plates", ***Materials & Design***, Vol. 30, No. 9, (2009), 3679-3685.
20. Sahraee, S., "Bending analysis of functionally graded sectorial plates using levinson plate theory", ***Composite Structures***, Vol. 88, No. 4, (2009), 548-557.
21. Aghdam, M., Shahmansouri, N. and Mohammadi, M., "Extended kantorovich method for static analysis of moderately thick functionally graded sector plates", ***Mathematics and Computers in Simulation***, Vol. 86, No., (2012), 118-130.
22. Saidi, A., Hejripour, F. and Jomehzadeh, E., "On the stress singularities and boundary layer in moderately thick functionally graded sectorial plates", ***Applied Mathematical Modelling***, Vol. 34, No. 11, (2010), 3478-3492.
23. Nosier, A. and Reddy, J., "On boundary layer and interior equations for higher-order theories of plates", ***ZAMM-Journal of Applied Mathematics and Mechanics/Zeitschrift für Angewandte Mathematik und Mechanik***, Vol. 72, No. 12, (1992), 657-666.
24. Nosier, A., Yavari, A. and Sarkani, S., "On a boundary layer phenomenon in mindlin-reissner plate theory for laminated circular sector plates", ***Acta Mechanica***, Vol. 151, No. 3-4, (2001), 149-161.
25. Mousavi, S.M. and Tahani, M., "Analytical solution for bending of moderately thick radially functionally graded sector plates with general boundary conditions using multi-term extended kantorovich method", ***Composites Part B: Engineering***, Vol. 43, No. 3, (2012), 1405-1416.
26. Fereidoon, A., Mohyeddin, A., Sheikhi, M. and Rahmani, H., "Bending analysis of functionally graded annular sector plates by extended kantorovich method", ***Composites Part B: Engineering***, Vol. 43, No. 5, (2012), 2172-2179.
27. Saidi, A., Jomehzadeh, E. and Atashipour, S., "Exact analytical solution for bending analysis of functionally graded annular sector plates", ***IJE Transactions***, Vol. 22, No. 3, (2009), 307-316.
28. Nasr, A., Atashipour, S.R. and Fadaee, M., "An elasticity solution for static analysis of functionally graded curved beam subjected to a shear force", ***International Journal of Engineering. Transactions B: Applications***, (2010), 169-178.
29. Kazerouni, S., Saidi, A. and Mohammadi, M., "Buckling analysis of thin functionally graded rectangulare plates with two opposite edges simply supported", ***International Journal of Engineering Transactions B: Applications***, Vol. 23, (2010), 179-192.
30. Golmakani, M. and Kadkhodayan, M., "Large deflection analysis of circular and annular fgm plates under thermo-mechanical loadings with temperature-dependent properties", ***Composites Part B: Engineering***, Vol. 42, No. 4, (2011), 614-625.
31. Golmakani, M., "Large deflection thermoelastic analysis of shear deformable functionally graded variable thickness rotating disk", ***Composites Part B: Engineering***, Vol. 45, No. 1, (2013), 1143-1155.
32. Golmakani, M. and Alamatian, J., "Large deflection analysis of shear deformable radially functionally graded sector plates on two-parameter elastic foundations", ***European Journal of Mechanics-A/Solids***, Vol. 42, (2013), 251-265.
33. Turvey, G. and Salehi, M., "Dr large deflection analysis of sector plates", ***Computers & Structures***, Vol. 34, No. 1, (1990), 101-112.
34. Reissner, E., "The effect of transverse shear deformation on the bending of elastic plates", (1945), 69-77.
35. Reddy, J.N., "Mechanics of laminated composite plates: Theory and analysis, CRC press, (1997).

36. Wang, C., Reddy, J.N. and Lee, K., "Shear deformable beams and plates: Relationships with classical solutions, Elsevier, (2000).
37. Dong, C., "Three-dimensional free vibration analysis of functionally graded annular plates using the chebyshev–ritz method", ***Materials & Design***, Vol. 29, No. 8, (2008), 1518-1525.
38. Bayat, M., Sahari, B., Saleem, M., Ali, A. and Wong, S.V., "Bending analysis of a functionally graded rotating disk based on the first order shear deformation theory", ***Applied Mathematical Modelling***, Vol. 33, No. 11, (2009), 4215-4230.
39. Ma, L. and Wang, T., "Nonlinear bending and post-buckling of a functionally graded circular plate under mechanical and thermal loadings", ***International Journal of Solids and Structures***, Vol. 40, No. 13, (2003), 3311-3330.
40. Day, A., "An introduction to dynamic relaxation(dynamic relaxation method for structural analysis, using computer to calculate internal forces following development from initially unloaded state)", ***The Engineer***, Vol. 219, (1965), 218-221.
41. Golmakani, M. and Kadkhodayan, M., "Nonlinear bending analysis of annular fgm plates using higher-order shear deformation plate theories", ***Composite Structures***, Vol. 93, No. 2, (2011), 973-982.
42. Golmakani, M. and Kadkhodayan, M., "An investigation into the thermoelastic analysis of circular and annular fgm plates", ***Mech Advanced Mater Struct***, Vol., No.
43. Turvey, G.J. and Salehi, M., "Annular sector plates: Comparison of full-section and layer yield predictions", ***Computers & Structures***, Vol. 83, No. 28, (2005), 2431-2441.
44. Falahatgar, S.R. and Salehi, M., "Dynamic relaxation nonlinear viscoelastic analysis of annular sector composite plate", ***Journal of Composite Materials***, Vol. 28, (2008), 2431-2441.
45. Salehi, M. and Sobhani, A., "Elastic linear and non-linear analysis of fiber-reinforced symmetrically laminated sector mindlin plate", ***Composite structures***, Vol. 65, No. 1, (2004), 65-79.
46. Zhang, L., Kadkhodayan, M. and Mai, Y.-W., "Development of the madr method", ***Computers & Structures***, Vol. 52, No. 1, (1994), 1-8.
47. Zhang, L. and Yu, T., "Modified adaptive dynamic relaxation method and its application to elastic-plastic bending and wrinkling of circular plates", ***Computers & Structures***, Vol. 33, No. 2, (1989), 609-614.

Non-linear Thermo-mechanical Bending Behavior of Thin and Moderately Thick Functionally Graded Sector Plates Using Dynamic Relaxation Method

M.E. Golmakani[a], M. Kadkhodayan[b]

[a] *Department of Mechanical Engineering, College of Engineering, Mashhad Branch, Islamic Azad University, Mashhad, Iran*
[b] *Department of Mechanical Engineering, Ferdowsi University of Mashhad, Mashhad, Iran*

PAPER INFO

Paper history:
Received 31 May 2015
Received in revised form 23 May 2016
Accepted 02 June 2016

Keywords:
Non-linear Bending
Functionally Graded Materials
Sector Plate
Thermo-mechanical Behavior
Dynamic Relaxation Method

چکیده

در این مقاله خمش غیر خطی قطاع صفحات تابعی توپر و حلقوی که در معرض یک بار مکانیکی عرضی و گرادیان دمایی در راستای ضخامت قرار دارند، بررسی شده است. خواص مواد مواد بطور پیوسته در راستای ضخامت صفحه بر اساس قانون توانی توزیع گشته‌اند. با استفاده از رابطه ون کارمن برای تغییر شکل-های بزرگ دو دستگاه معادلات تعادل غیر خطی بر اساس تئوری تغییر شکل‌های برشی مرتبه اول و تئوری کلاسیک استخراج گشته‌اند. برای حل این دستگاه معادلات از ترکیب روش‌های رهایی پویا و اختلاف محدود مرکزی استفاده شده است. بمنظور نشان دادن صحت ودقت پاسخ‌های بدست آمده از حل حاضر، چندین مطالعه مقایسه‌ای ارائه گشته است. اثرات شاخص تابعی ماده، شرایط مرزی، زاویه قطاع، نسبت ضخامت به شعاع و اختلاف دمایی مورد مطالعه قرار گرفته است. همچنین بمنظور بررسی اثر تغییر شکل‌های برشی و اهمیت تحلیل غیر خطی بر روی نتایج، برخی تحلیل‌های خطی و غیر خطی بر اساس هر دو تئوری برشی مرتبه اول و کلاسیک برای نسبت‌های مختلف ضخامت به شعاع و شرایط مرزی انجام شده است.

***doi**: 10.5829/idosi.ije.2016.29.06c.00*